

DOI: 10.1002/cctc.201300909

# Tuning the Selectivity in the Aerobic Oxidation of Cumene Catalyzed by Nitrogen-Doped Carbon Nanotubes

Shixia Liao, Yumei Chi, Hao Yu, Hongjuan Wang, and Feng Peng<sup>\*[a]</sup>

In this study it is demonstrated that carbon nanotubes (CNTs) with doped nitrogen atoms in graphitic domains (NCNTs) can act as a new class of metal-free catalysts exhibiting excellent activity in the aerobic oxidation of cumene. We proved that NCNTs can promote the decomposition of hydroperoxide cumene with exceptionally high activity, resulting in strongly increased cumene conversion and extraordinarily high selectivity to acetophenone and 2-benzyl-2-propanol. The incorporation of nitrogen altered the surface electron structure of the CNTs and tuned the reactivity and selectivity. DFT calculations

revealed that the remarkable improvement of catalytic performance of NCNTs is caused by the strong interaction between hydroperoxide cumene and the NCNTs. NCNTs also exhibited desirable recyclability after four cycling tests. This study not only provides a novel method for the cumene oxidation to high-value-added products at moderate reaction temperatures and oxygen atmospheric pressure, but also gives new insights into the effect of surface nitrogen doping on carbon-catalyzed liquid-phase oxidation of aromatic hydrocarbons.

## Introduction

As one of the most interesting metal-free catalysts, carbon materials have shown enormous promise in catalysis, owing to their physicochemical and mechanical properties, such as high surface areas, outstanding electron conductivity, corrosion resistance, and thermal stability.<sup>[1]</sup> Especially, carbon nanotubes (CNTs) have been widely explored as a new-generation catalyst in the oxidative dehydrogenation of hydrocarbons to corresponding olefins,<sup>[2]</sup> wet oxygen oxidation of phenolic water,<sup>[3]</sup> the selective oxidation of aldehydes, alcohols, or hydrocarbons,<sup>[4]</sup> and so on. One of the most prominent and high-industrial-relevance examples is the oxidative dehydrogenation of ethylbenzene. A widely accepted reaction mechanism proposes that rich-in-electron diketone-like carbonyl groups on the surface of carbon materials are the active sites.<sup>[2]</sup>

Some inorganic compounds and elements can be doped into graphitic carbon materials and provide a convenient means of fine-tuning the structure and reactivity. For example, nonmetal heteroatom doping (boron, sulfur, phosphorous, and nitrogen)<sup>[5]</sup> can change the band gap and thus influences electron (charge) mobility of carbons. In particular, substitutional N doping of nanographitic carbons has received intensive attention, because its outstanding performance in electrocatalysis has been theoretically predicted and experimentally observed.<sup>[6]</sup> Recently, it was found that the N atoms introduced at sp<sup>2</sup>-hybridized graphitic sites in the carbon framework could effectively enhance the activity of nanocarbon materials in the

aerobic oxidation of hydrocarbon.<sup>[7]</sup> In our previous work, we have proven that pristine CNTs can directly catalyze the aerobic oxidation of cyclohexane to adipic acid and their activities can be considerably improved by N doping.<sup>[7a,d]</sup> Ma and co-workers recently reported that N-doped sp<sup>2</sup>-hybridized layered carbons exhibits remarkably improved catalytic activity for ethylbenzene oxidation as well as a strongly increased acetophenone selectivity.<sup>[7b]</sup> However, there is a lack of clear knowledge on the mechanism of carbon-based liquid-phase catalysis for different reaction systems and the tuning mechanism of N doping on reactivity, thus, further studies are required.

The selective liquid-phase aerobic oxidation of cumene to hydroperoxide cumene (CHP) is extremely important in chemical industry, because CHP is an important intermediate in the production of phenol and acetone.<sup>[8]</sup> Today, more than 90% of the phenol in the world is produced by this route. Recently, it was reported that N-hydroxyphthalimide-cobalt acetate homogeneous catalysts could oxidize cumene to acetophenone (AP) and 2-benzyl-2-propanol (BP) with 80% selectivity and 35% conversion,<sup>[9]</sup> which are highly valuable intermediates in the manufacture of perfumes, pharmaceuticals, and resins.<sup>[10]</sup> Although this catalyst system is expensive and complicated to separate, it offers a possibility to change the existing complicated and environment-unfriendly BP synthesis process.<sup>[10d,11]</sup> The direct conversion of cumene to BP and AP is a very attractive route. To this end, it is of particular interest to know whether it is possible to tune cumene oxidation by heterogeneous carbon catalyst to obtain high-value-added products at moderate reaction temperatures and ambient pressure with oxygen as the oxidant.

Herein, we demonstrate that CNTs with nitrogen atoms doped into graphitic domains (NCNTs) can act as a new class of metal-free catalyst that can afford excellent activity in the

[a] S. Liao, Y. Chi, Dr. H. Yu, Dr. H. Wang, Prof. Dr. F. Peng  
School of Chemistry and Chemical Engineering  
South China University of Technology  
Guangzhou, Guangdong, 510640 (China)  
E-mail: cefpeng@scut.edu.cn

 Supporting information for this article is available on the WWW under <http://dx.doi.org/10.1002/cctc.201300909>.

aerobic oxidation of cumene. NCNTs were proven to promote the CHP decomposition with exceptionally high activity, resulting in a strongly increased cumene conversion and an extraordinarily high selectivity to BP and AP. By correlation of the activity with the surface structure of CNTs and further DFT calculations, a reasonable reaction network responsible for the liquid-phase oxidation of cumene on CNTs was proposed. This study not only provides a novel method for cumene oxidation to high-value-added products at moderate reaction temperatures and oxygen atmospheric pressure, but also gives new insights into the effect of surface N doping on carbon-catalyzed liquid-phase oxidation of aromatic hydrocarbons.

## Results and Discussion

N doping is an effective way to improve catalytic activity of carbon materials. To explore the special effect of N doping in cumene oxidation system, four different NCNTs with nitrogen contents in the range of 0.31–4.36 atom% were prepared by the chemical vapor deposition method with changing precursors and atmosphere. In Figure S1 (Supporting Information), the typical bamboo-like structures of NCNTs prepared with Fe catalyst are shown.<sup>[12]</sup> The concentration of N on the surface of samples was measured by X-ray photoelectron spectroscopy (XPS). As shown in Figure S2 and Table S1, the N/(N+C) atomic ratios on the surfaces of catalysts varied from 0.31% to 4.36% and different N functional groups were deconvoluted (see our previous article<sup>[7d]</sup>).

The effect of N doping on the cumene oxidation reaction is shown in Table 1. CNTs without N doping afforded 16.1% cumene conversion with 90.0% selectivity to CHP. Notably, N doping markedly promoted the activity, for example, NCNTs-3 exhibited the best catalytic performance, reaching 74.7% conversion after 8 h of reaction, which is 4.6 times that of undoped CNTs. This result strongly implies that the N doping indeed contributes to the considerable improvement of activity. More interestingly, with the content of nitrogen rising, the total selectivity to AP and BP increased distinctly from 10% to 96.7%,

whereas CHP selectivity decreased rapidly from 90.0% to 3.3%, and the distribution of products was changed completely. In addition, with the reaction time increasing, the conversion of cumene and total selectivity to AP and BP further increased. NCNTs-3 catalyst afforded 86% conversion of cumene and 99% selectivity to AP and BP after 24 h. To our knowledge, it is the first time that the cumene aerobic oxidation reaction can be altered to one-step production of BP and AP giving the total selectivity as high as 99% and a conversion higher than 80% under oxygen atmospheric pressure with the reaction temperature as low as 353 K, in the presence of metal-free catalyst.

To further discuss the relationship between catalytic performance and structure of NCNTs, we correlated the reaction rates with surface N loadings under the conversion of cumene controlled at approximately 20%. The reaction rates were respectively normalized by the BET surface area (Figure S3a) and catalyst mass (Figure 1a). The obtained data did not display a direct correlation between activity and surface area. Instead, the activity appeared to be more in-line with the N content. This phenomenon was also found in liquid-phase oxidation of ethylbenzene to acetophenone.<sup>[7b]</sup> As revealed in Figure 1a, the mass-normalized rate monotonously increased with total nitrogen content increasing, however, the linear correlation of activity with N contents was not possible because of the structural and morphological complexity of the synthesized NCNTs. The initial reaction rate rapidly increased, and then slowly increased after the N content was higher than 3.44%. For NCNTs-3 catalyst, the initial reaction rates normalized by catalyst mass and BET surface area were 10.4 and 3 times of those of the undoped CNTs, respectively. Nitrogen doping dramatically enhanced the catalytic activity of CNTs for cumene oxidation. As expected, the value of the apparent activation energy for oxidation of cumene was 12.8 kJ mol<sup>-1</sup> using NCNTs-3 as catalyst (see Figure S4), which is far lower than that for commercial CNTs (50.4 kJ mol<sup>-1</sup>), demonstrating that the oxidation of cumene is promoted by the N doping. The effects of different N species including quaternary (N<sub>Q</sub>), pyridinic (N<sub>P</sub>) and pyrrolic (N<sub>Pyr</sub>) nitrogen on the catalytic activity were similar to that of total N content (Figure 1b), however, the essential effect of various nitrogen forms in NCNTs on the catalytic activity remains not clearly distinguishable. The tuning role of nitrogen doping on products selectivity of cumene aerobic oxidation is also clearly revealed in Figure 1c. The BP/AP ratio rapidly decreased first, and then remained constant at 2.2 after the N content was higher than 3.44%.

The possibility that residual metal impurities are the active sites should be considered. In our work, all as-prepared

Catalyst	N/(N+C) [atom %]	S <sub>BET</sub> [m <sup>2</sup> g <sup>-1</sup> ]	X <sup>[b]</sup> [%]	Selectivity [%]			BP/AP <sup>[c]</sup>	r <sup>[c]</sup> [mmol m <sup>-2</sup> h <sup>-1</sup> ]	r <sup>[c]</sup> [mmol g <sup>-1</sup> h <sup>-1</sup> ]
				CHP	BP	AP			
CNTs	0.00	20.9	16.1	90.0	8.4	1.6	5.3	0.673	14.1
NCNTs-1	0.31	35.1	30.7	71.0	23.9	5.1	5.0	0.874	30.6
NCNTs-2	2.21	48.9	53.9	15.7	57.2	27.1	2.6	2.378	116.2
NCNTs-3	3.44	72.6	74.7	3.1	56.1	40.8	2.2	2.026	147.0
NCNTs-4	4.36	52.4	72.1	3.3	56.2	40.5	2.2	3.004	157.5
NCNTs-3 <sup>[d]</sup>	3.44	72.6	86.4	1.0	55.8	43.2	–	–	–
NCNTs-3 <sup>[e]</sup>	3.44	–	73.9	3.3	57.0	39.7	–	–	–
FeN <sub>x</sub> /NCNTs-3	3.44	–	64.9	7.4	54.0	38.6	–	–	–
NCNTs-3 <sup>[f]</sup>	3.44	72.6	0.1	–	–	–	–	–	–
blank <sup>[g]</sup>	–	–	2.7	99.2	0.4	0.4	–	–	–
blank <sup>[h]</sup>	–	–	3.2	93.9	5.6	0.5	–	–	–

[a] Reaction conditions: cumene (10 mL), catalyst (0.1 g), T = 353 K, t = 8 h, O<sub>2</sub> flow rate = 10 mL min<sup>-1</sup>; conversion and selectivity were determined by using GC and iodometry. [b] Conversion of cumene. [c] All conversions were controlled to nearly 20%. [d] Reaction for 24 h. [e] Without HCl treatment. [f] 2 wt% p-benzoquinone was added. [g] Without CHP and catalyst. [h] 2 wt% CHP was added without catalyst.

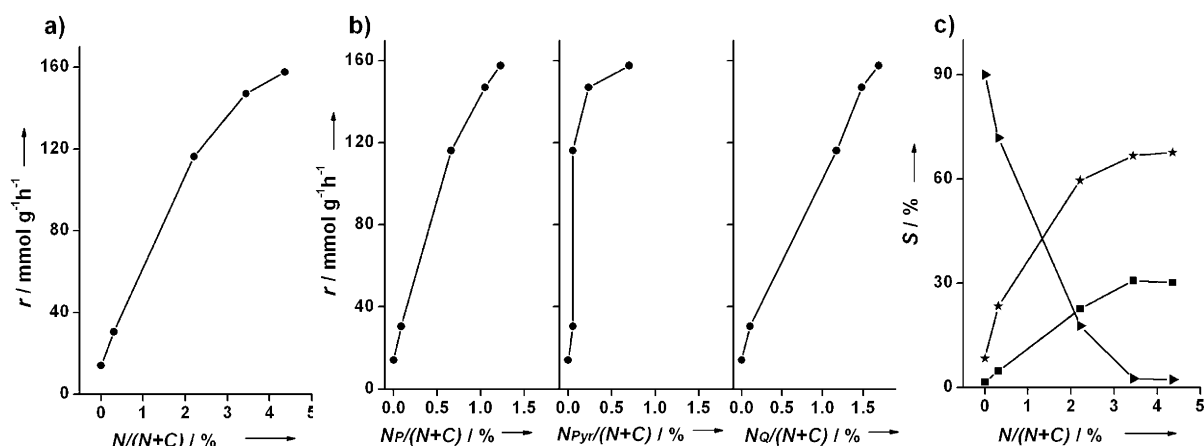


**Figure 1.** The dependences of mass-normalized reaction rates ( $r$ ) on a) the total N content, b) different N groups, and c) the effect of the nitrogen content on products distribution.  $N_p$  = pyridinic group,  $N_{pyr}$  = pyrrolic group,  $N_q$  = quaternary nitrogen. ●: Cumene reaction rate; ▲: CHP, ★: BP, and ■: AP selectivity. Reaction conditions: cumene 10 mL, catalyst 0.1 g, 353 K, O<sub>2</sub> flow rate of 10 mL min<sup>-1</sup>, the conversion and selectivity were determined by GC and iodometry. All conversions were controlled at approximately 20%.

carbon-based catalysts were washed in concentrated hydrochloric acid to remove the metal. As shown in Table 1, for NCNTs-3, no obvious changes in cumene conversion and products distribution were found compared with the NCNTs-3 untreated by HCl. In NH<sub>3</sub> atmosphere and at high temperature, metal nitrides could also be easily formed,<sup>[13]</sup> thus we prepared an FeN<sub>x</sub>-loaded NCNTs-3 catalyst (Table 1). A slightly decreased cumene conversion indicates that FeN<sub>x</sub> is not the active site, implying that the residual metal impurities do not play an active role in cumene oxidation under our reaction conditions.

It was widely accepted that cumene autoxidation undergoes a radical-involved reaction mechanism.<sup>[14]</sup> To prove the dominant role of radical species in our system, *p*-benzoquinone as a typical radical scavenger and CHP as a free-radical initiator were added to the reactant (see Table 1). After adding *p*-benzoquinone, the reaction was nearly totally prevented (NCNTs-3<sup>[b]</sup>), which indicates that cumene oxidation catalyzed by NCNTs is also a radical-involved reaction. For blank tests with or without addition of CHP, the conversion of cumene remained very low, possibly because CHP is stable at the reaction temperature. It can be concluded that CNTs play an important role in cumene oxidation.

Many researchers have discussed the detailed reaction process of cumene oxidation.<sup>[14b,15]</sup> Although the reaction network remains different in different catalysis systems, two approaches to the generation of important cumenyl radical (R<sup>•</sup>) have been commonly accepted in the chain-initiation process, namely the direct abstraction of H atom from cumene (denoted as RH) and the reaction of cumene with cumenyl oxygen radical (RO<sup>•</sup>) generated by the decomposition of CHP (also denoted as ROOH) as shown in Equations (1)–(3):



The CHP decomposition process could effectively accelerate the reaction rate of cumene and shorten the induction period. To discover the role of CHP in our system, the effect of different CNTs on the decomposition rate of CHP was investigated as shown in Table 2. Compared with the blank, CNTs obviously promoted the decomposition of CHP. Especially, for N-doped CNTs, the conversion of CHP rapidly increased with the content of nitrogen increasing. The decomposition products of CHP are AP and BP. After adding *p*-benzoquinone, the decomposition reaction of CHP was nearly totally prevented, indicating that CHP decomposition catalyzed by NCNTs is also a radical-involved reaction. In addition, the dependence of cumene conversion on CHP decomposition rate was determined (Figure S5), demonstrating that the cumene conversion increases with CHP decomposition rate increasing. Luz recently also reported that the decomposition ability of hydroperoxide on different catalysts was responsible for their catalytic oxidation activity of alkanes.<sup>[16]</sup> Hence, it was supposed that, if CHP decomposition is accelerated with NCNTs, more RO<sup>•</sup> and R<sup>•</sup> free radicals are generated, which will accelerate chain propagation reactions (discussed later in reaction mechanism).

**Table 2.** The performance of different CNTs for the decomposition of CHP.<sup>[a]</sup>

Catalyst	N/(N+C) [atom %]	<i>t</i> [h]	Conversion [%]	<i>r</i> [mmol g <sup>-1</sup> h <sup>-1</sup> ]
–	–	4	5.5	1.6
CNTs	0.00	4	13.4	3.9
NCNTs-1	0.31	4	52.3	25.0
NCNTs-2	2.21	1	80.7	92.8
NCNTs-3	3.44	0.4	97.5	280.3
NCNTs-4	4.36	0.4	97.8	281.1
NCNTs-3 <sup>[b]</sup>	3.44	1	0	0

[a] Reaction conditions: CHP (2 g), catalyst (0.1 g), acetonitrile as solvent (8 mL), *T* = 353 K. The conversion was determined by using iodometry. The decomposition products were exclusively AP and BP. [b] 2 wt % *p*-benzoquinone was added.

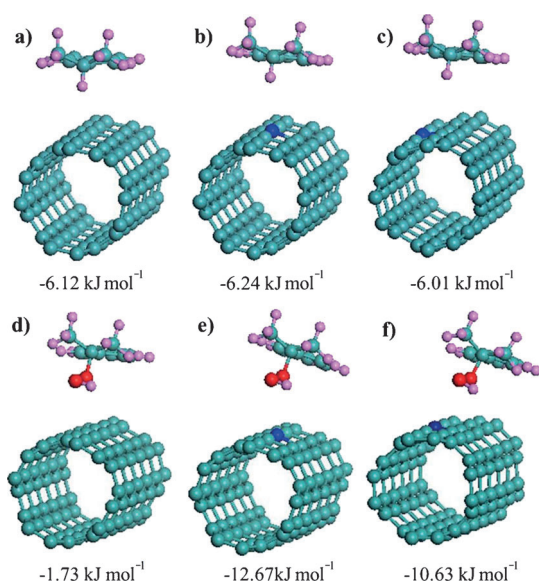


**Figure 2.** Optimized structures and adsorption energies of a–c) cumene and d–f) CHP on the surface of a, d) CNT; b, e) N site of NCNT; and c, f) adjacent C site of NCNT. ●: C, ●: O, ●: N, ●: H.

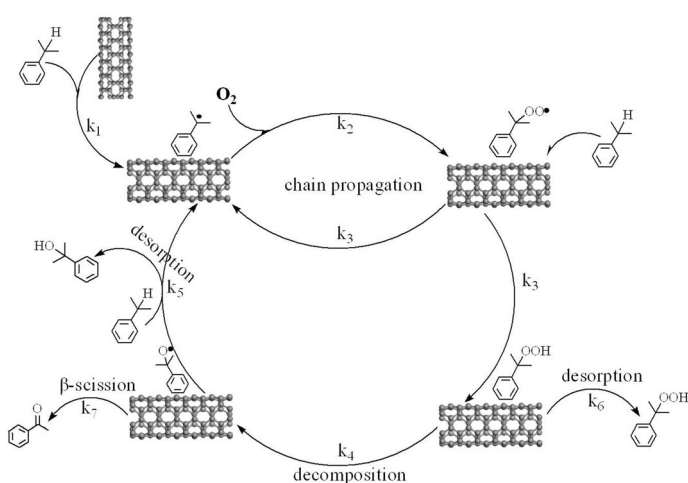
Electron-donating nitrogen doped into in graphitic domains was reported to facilitate the adsorption of reactive intermediates and thus improve the electrocatalysis of oxygen reduction.<sup>[17]</sup> To get more insights into the structure–property relationship, the first-principle DFT was used to calculate the adsorption energies of reactant and radicals on CNTs and NCNTs. The CNT model is in perfect arm-chair structure without defects. NCNT represents the CNT with one carbon atom replaced by quaternary N. As shown in Figure 2, the adsorption of reactant and radicals on both CNT and NCNT is energetically favorable. This can be ascribed to the conjugation effect between the benzene ring of the aromatic hydrocarbon and the graphene  $\pi$ -system.<sup>[18]</sup> After N doping, the adsorption energies of cumene and  $R^{\bullet}$  are evidently unchanged. However, the adsorption energy of CHP prominently declines from  $-1.73 \text{ kJ mol}^{-1}$  to  $-12.67 \text{ kJ mol}^{-1}$  after N doping, indicating that the interac-

tion between CHP and CNTs is strengthened largely, which is consistent with the better catalytic performance of NCNTs in CHP decomposition. Similarly, the oxygenous free radicals ( $RO^{\bullet}$  and  $ROO^{\bullet}$ ) are also more easily adsorbed on the NCNT, as shown in Figure S6. The appropriate interaction would be beneficial for the chain-propagation process and the formation of AP and BP. This can well explain the role of N doping.

Based on above data, a possible reaction network is proposed as shown in Scheme 1. 1) At the initial stage, cumene is adsorbed on the surface of CNTs by the  $\pi$ - $\pi$  conjugation effect between the hexatomic ring of CNTs and the benzene ring of cumene. As no initiator is added,  $R^{\bullet}$  radical is formed through H abstraction of cumene at a low rate of  $k_1$ . Then the chain-propagation process starts: the direct interaction between oxygen and the formed  $R^{\bullet}$  radical to produce the cumyl peroxy radical ( $ROO^{\bullet}$ ) ( $k_2$ ), followed by hydrogen abstraction from cumene to produce CHP and  $R^{\bullet}$  radical ( $k_3$ ). 2) Once CHP is produced, some of the CHP molecules are adsorbed on the surface of CNTs and the others are desorbed as final product ( $k_6$ ). As CNTs can accelerate the electron-transfer-induced decomposition of hydroperoxides,<sup>[19]</sup> the adsorbed CHP molecules are more inclined to decompose into  $RO^{\bullet}$  ( $k_4$ ), which can easily abstract a H atom of cumene to form  $R^{\bullet}$  and BP ( $k_5$ ). The formed  $R^{\bullet}$  continues to enter the chain-propagation process. At the same time, AP is produced through the  $\beta$ -scission of  $RO^{\bullet}$  ( $k_7$ ).

For pristine CNTs, the formed CHP is more inclined to desorb from the surface of tubes, and only a small proportion is adsorbed and further decomposed for the new cycle. As an incorporated N atom has one more electron than carbon, which can increase the charge density in addition to the conjugated  $\pi$ -bond system,<sup>[6a,20]</sup> the formed CHP is easily adsorbed on the surface of NCNTs, which is demonstrated by the lower adsorption energy. At the same time, the electron-transfer-induced decomposition reaction of CHP is improved dramatically with the enhancement of charge density. Therefore, more  $RO^{\bullet}$  and  $R^{\bullet}$  free radicals are generated, leading to a higher reaction rate and BP concentration. With the accumulation of  $RO^{\bullet}$  and possible enhanced interaction between  $RO^{\bullet}$  and NCNTs, more AP is also produced. The concentration of CHP remains at a low level owing to its rapid decomposition. These results well explain the differences of catalytic activity and products distribution between CNTs and NCNTs.

In addition to the remarkable catalytic performance, the good stability of CNTs as catalysts is also an advantage (Figure 3). Taking the NCNTs-3 catalyst, for example, after four cycles, no obvious difference in both cumene conversion and product distributions was found. The  $I_D/I_G$  ratio in Raman spectroscopy (Figure S7) and the morphology (Figure 4) of the catalyst were obviously unchanged after recycling. These results strongly indicate that NCNTs are very active and stable catalysts for the oxidation of cumene. Therefore, it is promising to produce AP and BP with NCNTs catalysts through cumene liquid aerobic oxidation in industry.



**Scheme 1.** Reaction network of cumene with CNTs as catalysts.

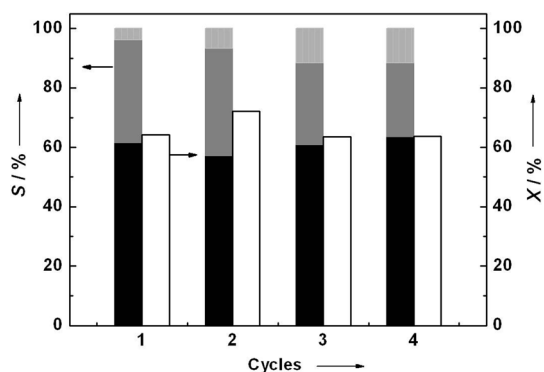


**Figure 3.** Reuse of NCNTs-3 catalyst. Reaction conditions: cumene 10 mL, O<sub>2</sub> flow rate 10 mL min<sup>-1</sup>, 353 K, 8 h. □: Cumene conversion; ■: BP, ▒: AP, and ■: CHP selectivity.

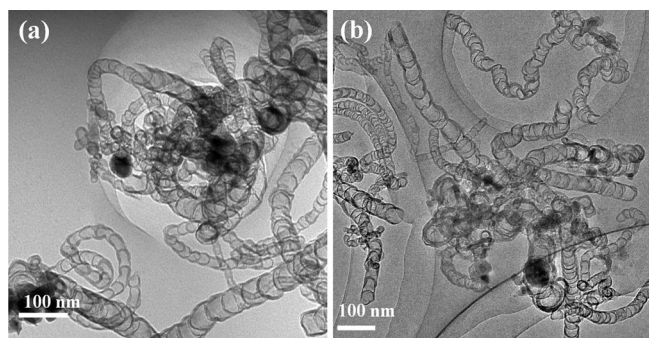


**Figure 4.** TEM images of NCNTs-3 a) before reaction and b) after the 4th cycle.

## Conclusions

We have demonstrated that carbon nanotubes with the nitrogen atoms doped into graphitic domains as a new class of metal-free catalyst can afford an excellent activity in the aerobic oxidation of cumene. We proved that nitrogen-doped carbon nanotubes can promote the hydroperoxide cumene decomposition with exceptionally high activity, resulting in a highly increased cumene conversion and an extraordinarily high selectivity to 2-benzyl-2-propanol and acetophenone. The incorporation of nitrogen altered the surface electron structure of the carbon nanotubes and tuned the reactivity and selectivity. DFT calculations revealed that the remarkable improvement of catalytic performance of nitrogen-doped carbon nanotubes is caused by the strong interaction between hydroperoxide cumene and carbon nanotubes. Based on these results, a possible reaction network was given. In addition, nitrogen-doped carbon nanotubes showed good recyclability in cumene oxidation. This study not only provides a novel method for cumene oxidation to high-value-added products at a moderate reaction temperature and oxygen atmospheric pressure, but also gives new insight into the effect of surface nitrogen doping on carbon-catalyzed liquid-phase oxidation reaction of aromatic hydrocarbons.

## Experimental Section

### Preparation

The NCNTs were synthesized by a chemical vapor deposition method in a horizontal tubular quartz furnace with 4 cm inner diameter over FeMo/Al<sub>2</sub>O<sub>3</sub> catalyst. The details of the FeMo/Al<sub>2</sub>O<sub>3</sub> catalyst can be found in Ref. [21]. To obtain NCNTs with different N contents, 10 mL mixtures of xylene and aniline with different aniline volume percentage were injected by a syringe pump at a rate of 3 mL h<sup>-1</sup>. The liquid mixtures were vaporized in the quartz tube at approximately 353 K. The growth of NCNTs was performed at 1073 K in Ar or NH<sub>3</sub> at 500 cm<sup>3</sup> min<sup>-1</sup>.<sup>[8d]</sup> NCNT-1 and NCNT-2 were denoted as N-doped carbon nanotubes prepared in Ar with 10% and 100% (v/v) of aniline in the precursors, respectively. NCNTs-3 and NCNTs-4 were denoted as N-doped carbon nanotubes prepared in NH<sub>3</sub> with 0% and 100% (v/v) of aniline in precursors, respectively. As a comparison, we also prepared nitrogen-free carbon nanotubes under the same conditions with xylene as precursor in Ar, denoted as CNTs. The residual FeMo/Al<sub>2</sub>O<sub>3</sub> catalyst in all obtained CNTs was removed by washing with 12 mol L<sup>-1</sup> HCl aqueous solution before catalytic tests and characterizations. The commercial CNTs were purchased from Shenzhen Nanotech Port Co. Ltd (NTP) and also purified with above method.

### Characterizations

BET specific surface areas were measured by N<sub>2</sub> adsorption at liquid N<sub>2</sub> temperature in an ASAP 2010 analyzer. Raman spectra were obtained in a LabRAM Aramis micro Raman spectrometer with an excitation wavelength at 532 nm with 2 μm spot size. TEM images were obtained with a FEI Tecnai G2 12 microscope operated at 100 kV and a JEOL JEM2010 microscope operated at 200 kV. Specimens for TEM and HRTEM were prepared by ultrasonically suspending the sample in acetone and depositing a drop of the suspension onto a grid. XPS analysis was performed in a Kratos Axis ultra (DLD) spectrometer equipped with an AlK<sub>α</sub> X-ray source in ultrahigh vacuum (< 133 × 10<sup>-10</sup> Pa). The binding energies (± 0.2 eV) were referenced to the C 1s peak at 284.6 eV. The surfaces of samples were cleaned by heat treatment at 373 K in ultrahigh vacuum prior to the measurements.

### Calculations

All results were calculated by using Cambridge Sequential Total Energy Package codes, implemented in Materials Studio environment.<sup>[22]</sup> Exchange–correlation function was the popular Perdew–Burke–Ernzerhof generalized gradient approximation.<sup>[23]</sup> The interactions were described by norm-conserving pseudopotentials. Lattice constants of the cell were 18, 18, and 14 Å, respectively. A plane wave basis set with a cutoff energy of 300 eV was used. K-point sampling was restricted to a single point. Models used in this work were single-walled arm-chair nanotubes with 96 atoms. The adsorption energy ( $E_{\text{ads}}$ ) was defined as the total energy gained by molecule adsorption at equilibrium distance, as shown in Equation (4).<sup>[24]</sup>

$$E_{\text{ads}} = E_{\text{tube+molecule}} - E_{\text{tube}} - E_{\text{molecule}} \quad (4)$$

### Catalytic tests

The liquid oxidation reactions were performed in a three-necked flask (20 mL), supplied with a magnetic stirrer, reflux condenser, and an oil bath. Cumene (10 mL) and catalyst (100 mg) were put into the flask, sonicated for 5 min, and heated to the preconcerted temperature. Then oxygen was passed through the solution by bubbling at the temperature until the reaction was over. The CHP concentration was determined according to the iodometric method.<sup>[25]</sup> After the reduction of generated CHP to BP through the triphenylphosphine reaction,<sup>[26]</sup> the other products in the liquid phase were detected by gas chromatography (Agilent GC-6820) equipped with a 30 m × 0.25 mm × 0.25 μm HP-5 capillary column and a flame ionization detector (detector temperature 553 K, injector temperature 553 K, and oven temperature 413 K) using toluene as external standard.

The thermolysis tests of CHP were conducted according to reference.<sup>[19]</sup> Acetonitrile (8 mL) and catalyst (0.1 g) were added in a flask, sonicated for 5 min, and then placed in an oil bath at 353 K. After flushing with N<sub>2</sub> for 5 min, CHP (2 g) was added and the reaction was conducted in a closed system. The unreacted CHP was tested by the aforementioned iodometric method.

### Acknowledgements

This work was supported by the National Natural Science Foundation of China (No. 21133010, 21273079), the Guangdong Provincial Natural Science Foundation (No. S20120011275) and Program for New Century Excellent Talents in Universities of China (NCET-12-0190).

**Keywords:** carbon · doping · oxidation · nanotubes · nitrogen

- [1] a) J. Planeix, N. Coustel, B. Coq, V. Brotons, P. Kumbhar, R. Dutartre, P. Geneste, P. Bernier, P. Ajayan, *J. Am. Chem. Soc.* **1994**, *116*, 7935–7936; b) P. Serp, E. Castillejos, *ChemCatChem* **2010**, *2*, 41–47; c) D. S. Su, J. Zhang, B. Frank, A. Thomas, X. Wang, J. Paraknowitsch, R. Schlögl, *ChemSusChem* **2010**, *3*, 169–180.
- [2] a) D. Su, N. I. Maksimova, G. Mestl, V. L. Kuznetsov, V. Keller, R. Schlögl, N. Keller, *Carbon* **2007**, *45*, 2145–2151; b) X. Liu, D. S. Su, R. Schlögl, *Carbon* **2008**, *46*, 547–549; c) J. Zhang, X. Liu, R. Blume, A. Zhang, R. Schlögl, D. S. Su, *Science* **2008**, *322*, 73–77.
- [3] S. Yang, X. Li, W. Zhu, J. Wang, C. Descorme, *Carbon* **2008**, *46*, 445–452.
- [4] a) B. Frank, R. Blume, A. Rinaldi, A. Trunschke, R. Schlögl, *Angew. Chem.* **2011**, *123*, 10408–10413; *Angew. Chem. Int. Ed.* **2011**, *50*, 10226–10230; b) J. Luo, F. Peng, H. Yu, H. Wang, *Chem. Eng. J.* **2012**, *204*–206, 98–106; c) J. Luo, F. Peng, H. Yu, H. Wang, W. Zheng, *ChemCatChem* **2013**, *5*, 1578–1586.
- [5] a) V. Strelko, V. Kuts, P. Thrower, *Carbon* **2000**, *38*, 1499–1503; b) C. H. Choi, S. H. Park, S. I. Woo, *Green Chem.* **2011**, *13*, 406–412.
- [6] a) S. Maldonado, S. Morin, K. J. Stevenson, *Carbon* **2006**, *44*, 1429–1437; b) S. Kundu, T. C. Nagaiah, W. Xia, Y. Wang, S. V. Dommele, J. H. Bitter, M. Santa, G. Grundmeier, M. Bron, W. Schuhmann, *J. Phys. Chem. C* **2009**, *113*, 14302–14310; c) R. Li, W. Ji, J. Lin, *Phys. Rev. B* **2007**, *76*, 195406; d) X. Hu, Y. Wu, H. Li, Z. Zhang, *J. Phys. Chem. C* **2010**, *114*, 9603–9607.
- [7] a) H. Yu, F. Peng, J. Tan, X. Hu, H. Wang, J. Yang, W. Zheng, *Angew. Chem.* **2011**, *123*, 4064–4068; *Angew. Chem. Int. Ed.* **2011**, *50*, 3978–3982; b) Y. Gao, G. Hu, J. Zhong, Z. Shi, Y. Zhu, D. S. Su, J. Wang, X. Bao, D. Ma, *Angew. Chem.* **2013**, *125*, 2163–2167; *Angew. Chem. Int. Ed.* **2013**, *52*, 2109–2113; c) J. Long, X. Xie, J. Xu, Q. Gu, L. Chen, X. Wang, *ACS Catal.* **2012**, *2*, 622–631; d) Y. Cao, H. Yu, J. Tan, F. Peng, H. Wang, J. Li, W. Zheng, N.-B. Wong, *Carbon* **2013**, *57*, 433–442; e) J. Luo, F. Peng, H. Wang, H. Yu, *Catal. Commun.* **2013**, *39*, 44–49.
- [8] S. Matsui, T. Fujita, *Catal. Today* **2001**, *71*, 145–152.
- [9] K. Novikova, M. Kompanets, O. Kushch, S. Kobzev, M. Khliestov, I. Opeida, *React. Kinet. Mech. Catal.* **2011**, *103*, 31–40.
- [10] a) S. Devika, M. Palanichamy, V. Murugesan, *Appl. Catal. A* **2011**, *407*, 76–84; b) G. Yang, Y. Ma, J. Xu, *J. Am. Chem. Soc.* **2004**, *126*, 10542–10543; c) J.-Y. Qi, H.-X. Ma, X.-J. Li, Z.-Y. Zhou, M. C. Choi, A. S. Chan, Q.-Y. Yang, *Chem. Commun.* **2003**, 1294–1295; d) H.-Y. Hou, T.-S. Liao, Y.-S. Duh, C.-M. Shu, *J. Therm. Anal. Calorim.* **2006**, *83*, 167–171.
- [11] C. E. Frank, W. E. Foster, *Ind. Eng. Chem.* **1954**, *46*, 1019–1021.
- [12] S. Van Dommele, A. Romero-Izquierdo, R. Brydson, K. De Jong, J. Bitter, *Carbon* **2008**, *46*, 138–148.
- [13] S. Kurian, N. Gajbhiye, *Mater. Lett.* **2011**, *65*, 3089–3091.
- [14] a) K. Hattori, Y. Tanaka, H. Suzuki, T. Ikawa, H. Kubota, *J. Chem. Eng. Jpn.* **1970**, *3*, 72–78; b) A. Bhattacharya, *Chem. Eng. J.* **2008**, *137*, 308–319.
- [15] Y. F. Hsu, C. P. Cheng, *J. Mol. Catal. A* **1998**, *136*, 1–11.
- [16] I. Luz, A. León, M. Boronat, F. X. Llabrés i Xamena, A. Corma, *Catal. Sci. Technol.* **2013**, *3*, 371–379.
- [17] a) R. Liu, D. Wu, X. Feng, K. Müllen, *Angew. Chem.* **2010**, *122*, 2619–2623; b) K. Gong, F. Du, Z. Xia, M. Durstock, L. Dai, *Science* **2009**, *323*, 760–764.
- [18] W. Chen, L. Duan, D. Zhu, *Environ. Sci. Technol.* **2007**, *41*, 8295–8300.
- [19] P. S. Engel, W. E. Billups, D. W. Abmayr, K. Tsvaygboym, R. Wang, *J. Phys. Chem. C* **2008**, *112*, 695–700.
- [20] C. V. Rao, C. R. Cabrera, Y. Ishikawa, *J. Phys. Chem. Lett.* **2010**, *1*, 2622–2627.
- [21] W. Qian, H. Yu, F. Wei, Q. Zhang, Z. Wang, *Carbon* **2002**, *40*, 2968–2970.
- [22] M. Segall, P. J. Lindan, M. Probert, C. Pickard, P. Hasnip, S. Clark, M. Payne, *J. Phys. Condens. Matter* **2002**, *14*, 2717.
- [23] J. P. Perdew, K. Burke, M. Ernzerhof, *Phys. Rev. Lett.* **1996**, *77*, 3865.
- [24] J. Zhao, J. P. Lu, J. Han, C.-K. Yang, *Appl. Phys. Lett.* **2003**, *82*, 3746.
- [25] J. Zawadiak, D. Gilner, Z. Kulicki, S. Baj, *Analyst* **1993**, *118*, 1081–1083.
- [26] V. Y. Kugel, M. Tsodikov, G. Bondarenko, Y. V. Slivinskii, D. Kochubey, M. Hidalgo, J. Navio, *Langmuir* **1999**, *15*, 463–468.

Received: October 23, 2013

Revised: November 26, 2013

Published online on January 17, 2014